Determining the partial pressure of volatile components via substrate-integrated hollow waveguide infrared spectroscopy with integrated microfluidics.

Vjekoslav Kokoric, Johannes Theisen, Andreas Wilk, Christophe Penisson, Gabriel Bernard, Boris Mizaikoff, Jean Christophe Gabriel

Determining the Partial Pressure of Volatile Components via Substrate-Integrated Hollow Waveguide Infrared Spectroscopy with Integrated Microfluidics

Vjekoslav Kokoric,[1‡] Johannes Theisen,[2‡] Andreas Wilk,[1‡] Christophe Penisson,[2‡] Gabriel Bernard,[2] Boris Mizaikoff[1*] and Jean-Christophe P. Gabriel[3*]

1. Ulm University, Institute of Analytical and Bioanalytical Chemistry, Albert-Einstein-Allee 11, 89081 Ulm, Germany

2. ICSM, CEA/CNRS/UM2/ENSCM UMR5257, CEA Grenoble, 17 Avenue des Martyrs, 38000 Grenoble, France

3. CEA/DRF, 17 Avenue des Martyrs, 38054 Grenoble Cedex 09.

ABSTRACT: A microfluidic system combined with substrate-integrated hollow waveguide (iHWG) vapor phase infrared spectroscopy has been developed for evaluating the chemical activity of volatile compounds dissolved in complex fluids. Chemical activity is an important yet rarely exploited parameter in process analysis and control. Access to chemical activity parameters enables systematic studies on phase diagrams of complex fluids, the detection of aggregation processes, etc.. The instrumental approach developed herein uniquely enables controlled evaporation/permeation from a sample solution into a hollow waveguide structure, and analyzing the partial pressures of volatile constituents. For the example of a binary system, it was shown that the chemical activity may be deduced from partial pressure measurements at thermodynamic equilibrium conditions. The combined microfluidic-iHWG mid-infrared sensor system (μFLUID-IR) allows realizing such studies in absence of any perturbations provoked by sampling operations, which is unavoidable using state-of-the-art analytical techniques such as headspace gas chromatography. For demonstration purposes, a water-ethanol mixture was investigated, and the derived data was cross-validated with established literature values at different mixture ratios. Next to perturbation-free measurements, a response time of the sensor <150 seconds (t_{90}) at a recovery time <300 seconds (t_r) has been achieved, which substantiates the utility of μFLUID-IR for future process analysis-and-control applications.

INTRODUCTION

Industrial processes increasingly rely on complex fluid handling. However, detailed understanding on such fluid behavior frequently remains empirical due to their many constituents. In order to improve mechanistic understanding, new multiscale simulation packages are required. The latter development is especially difficult at mesoscale dimensions, since molecule aggregation, interface structures and system behavior are yet to be fully understood in most cases. However, a signature of aggregation can be found within solvent activity variations. Activity therefore becomes an important parameter, which advanced modelling packages are required to simulate.[1,2] Hence, there is a definite need to reliably measure and analyze chemical activity for each volatile component in such complex mixtures. To achieve this goal, the most straightforward approach is to measure partial pressures of all chemicals, and to follow their changes as a function of time and concentration.

Surprisingly, to the best of our knowledge, following chemical activities to study complex fluid behavior has yet to be performed and exploited routinely and in real-time. We attribute the lack of reports on this highly relevant aspect to the technical difficulties of the associated experimental setup. Yet, such analyses would be a major breakthrough in advancing fundamental understanding and modelling of these fluids, as well as real-time process monitoring. In particular, chemical processes associated with any separation plant, controlled crystallization reactors, or purification/recycling systems such as complex alcohol pertraction for "rectification" in distilleries, alcohol aggregation[3] or water activity to track monoclonal antibody agglomeration (a $141 bn market in 2017) would benefit from such capabilities.

Direct and (near) real-time measurement of chemical activity of volatile components remains challenging, however, may be derived from the measurement of equilibrium partial pressures according to Raoult's law. Notwithstanding, the partial pressures are correlated to the infrared absorbance of vapor phase constituents. A more precise description of the physicochemical relations between absorbance, partial pressures, and activities is given in the discussion section of this study.

In order to measure absorbance and to relate it to partial pressures, optical techniques such as conventional infrared

spectroscopy (IR), tunable diode laser spectroscopy (TDLS), laser induced breakdown spectroscopy (LIBS), etc. have been used.[4,5] In particular, Fourier transform infrared spectroscopy (FTIR) is a fast and nondestructive method enbaling simultaneous detection of several vapor phase species based on their roto-vibrational absorptions. Moreover, the sensitivity of IR absorption spectroscopic and sensing techniques may be tailored via adjusting the absorption path length, e.g., via using commercial multi-pass gas cells. However, such gas cell assemblies (e.g., White cells or Herriott cells) are bulky and require sizeable sample volumes up to a few liters, thereby considerably increasing equilibrium times and limiting their use for transient or real-time experiments. [5–7]

Indeed, when compared to other gas sensing technologies such as nanosensors[8,9] or nano-electro-mechanical systems (NEMS)[10], substrate-integrated hollow waveguide (iHWG) based FTIR analytical technology has recently emerged as a capable tool for probing minute gaseous sample volumes, i.e., few hundreds of microliters with high molecular selectivity. Therefore, iHWGs are an attractive alternative to conventional multi-pass gas cells not only offering an efficient photon conduit, but also a small device footprint (i.e., few square centimeters).[11] iHWGs are therefore nowadays considered as next-generation light pipe structures, simultaneously serving as a waveguide and a highly miniaturized, reliable and robust gas cell.[11,12]

In the present study, we report an innovative approach for chemical activity measurements of individual sample constituents by integrating a microfluidic cartridge and a liquid-vapor sampling cell based on iHWG technology for rapid equilibration, and combination with an FTIR spectrometer. For demonstrating the utility of the system, data are recorded for ethanol/water mixtures ranging from 0% to 100% ethanol (EtOH) content. The obtained results are consistent with established literature values, which renders the developed method the first easy-to-use tool for directly addressing solution activity via vapor phase measurements.

EXPERIMENTAL

MICROFLUDIC IR-IHWG ASSEMBLY

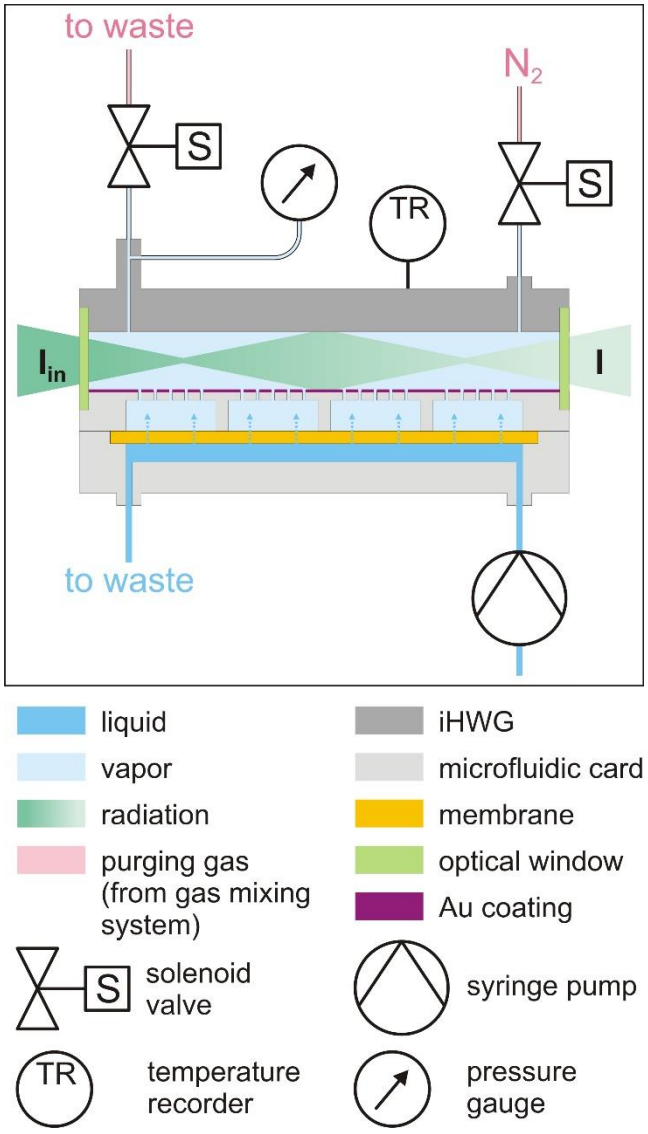

Fig. 1. Schematic cross-section of the experimental setup (not to scale). I_{in}: intensity of the in-coupled radiation (emanating from the FTIR spectrometer). Snapshot during the acquisition of a single-channel sample spectrum (i.e., both solenoid valves closed; equilibration phase). I: out-coupled radiation intensity; $I < I_{in}$ due to the presence of absorbing molecules within the IR beam path within the iHWG.

A schematic cross-section of the sandwiched microfluidic card and iHWG device developed in this study is shown in Figure 1. During operation, the liquid under investigation is fed into the microfluidic channel (here, bottom layer). All components of the condensed phase with non-negligible vapor pressure then evaporate – as indicated by dotted arrows – via a porous membrane into an intermediate void layer (i.e., vapor diffusion cell), and subsequently diffuse through perforations into the actual vapor cell (i.e., the light-guiding channel of the iHWG; here, top layer) sampled by IR radiation. In particular, the scheme in Figure 1 shows

a snapshot during a measurement routine with both solenoid valves closed, thus allowing for the establishment of equilibrium conditions within a fixed volume according to the compounds saturation vapor pressure. Also indicated in Figure 1 is the mid-infrared (MIR; 2 – 20 µm) radiation emanating from an FTIR spectrometer, which probes the waveguide/vapor cell, and eventually yields the intensity reading $I(\lambda)$ corresponding to the transmitted fraction incident at the semiconductor detector.

For absorption measurements, the likewise required intensity reading $I_0(\lambda)$ (cf. equation 4), i.e., the background or reference single-channel (RSC) is obtained while flushing the iHWG with nitrogen. Although evaporation through the membrane continues naturally, employing a sufficiently high N_2 flow rate ensures that all analyte concentrations within the waveguide are kept at negligible levels throughout the RSC spectra acquisition. Note that analyte concentrations may still be higher in the vapor diffusion cell, as indicated in Figure S1 (supporting information).

The microfluidic cartridge (see Fig. 1) is of credit card dimensions (85.60 mm × 53.98 mm × 10 mm) and made of poly(methyl methacrylate) (PMMA). To provide the microfluidic channel, a groove (36 mm × 2 mm × 0.4 mm) is milled into the bottom part providing a volume of approx. 20 µL. The channel is interfaced with external tubing using microfluidic connectors. The channel is closed off by a commercial oleophobic and hydrophobic porous PTFE membrane (thickness t = 190 µm, pore size d = 50 nm, porosity p ~ 70%, tortuosity τ ~ 2) acting as capillary barrier, indicated as yellow layer in Fig. 1. Following basic theory of molecular diffusion in porous media, the membrane non-specifically modifies vapor diffusion coefficients D to Deff = D p / τ ~ 0.3 D.[13] This is unspecific regarding molecules, since water, ethanol and dinitrogen are far smaller than pore diameter. The top PMMA part of the same lateral dimensions as the bottom part is made of 3 mm thick PMMA. It is milled to establish a vapor diffusion cell above the fluidic channel, as well as 0.4 mm wide apertures providing access to the iHWG component. 50 of these apertures make up for approx. 6% of total IR-exposed surface area on the PMMA component, and ensure rapid equilibrium between the liquid and the vapor phase while ensuring sufficient throughput of the reflected IR radiation (ray-tracing simulations estimated a transmission of ~ 90%; compare Fig. S2, supporting information). The top part closes off the iHWG, and is therefore metallized with a 100 nm gold coating (see Fig. 1 purple color) for maximizing the IR reflectivity. The microfluidic cartridge consists of bottom part, the membrane, and the top part assembled by bolts/nuts and sealed by silicone rubber ensuring liquid and gas tightness.

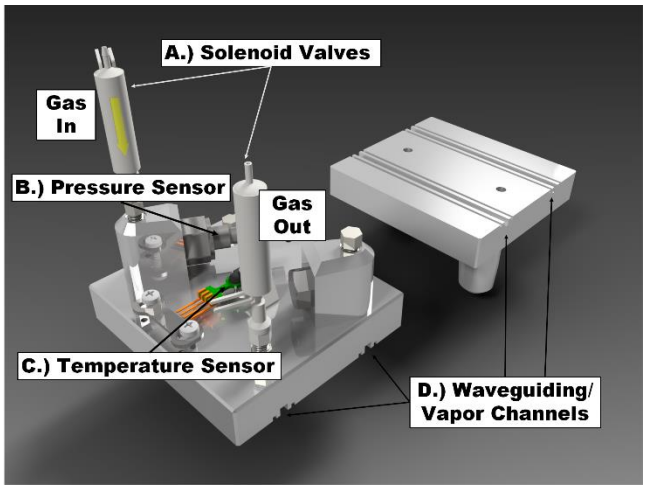

Figure 2: iHWG: (A) solenoid valves, (B) pressure sensor, (C) temperature sensor, and (D) waveguiding/vapor channels.

The key component of the system is the iHWG (Fig. 2), which constitutes the top part of the microfluidic cartridge. It should be noted that the assembly described herein actually comprised two iHWG channels with corresponding vapor transfer cell, membrane, and microfluidic channel enabling future simultaneous studies. However, in the present study only one channel was used for data acquisition.

The polished waveguiding/vapor cell (see Fig. 2 **(D)**) is integrated into a 53.98 × 50 mm aluminum substrate providing an absorption path length of approx. 54 mm. Throughout the entire spectrum acquisition period, the temperature of the device is monitored via a temperature sensor (SHT71, Sensirion AG, Switzerland) attached to the top face of the iHWG (compare Fig. 2 (**C**)).

Furthermore, the microfluidic/iHWG used in this study allows an optional pressure gauge to be mounted, which is only required if the ambient pressure is not constant (see Fig. 2 (**B**)). Thereby, the absolute pressure within the iHWG channel is directly accessible. Two miniature solenoid valves are installed at the gas inlet and outlet ports for purging nitrogen, and for alternatively sealing the device against the ambient environment. Finally, each end of the channel is sealed gas-tight via two IR transparent windows (BaF_2; thickness: 0.5 mm) glued by silicon rubber. The waveguiding/vapor cell channel is of 2 × 2.1 mm^2 cross-section and encloses a volume of approx. 226 µL. Two centering pins are used to align the iHWG and the PMMA top plate, which are then glued and sealed by epoxy resin. Two overflow channels prevent contamination of the optical path with redundant epoxy resin.

To generate different but constant and adjustable temperatures, the entire setup shown in Figure 3 was placed inside a climate chamber (IPP750 plus, Memmert, Germany). Throughout all experiments perfromed in the present study, a constant temperature of 20°C ± 0.1°C was maintained. The microfluidic IR-iHWG assembly (Fig. 3 **(C)**) was optically coupled to the FTIR spectrometer (Fig. 3 **(A)**) (Bruker Alpha OEM, Bruker Optics Inc., Ettlingen, Germany) using an off-axis parabolic mirror (OAPM) (Fig. 3 **(B)**) (MPD229-M01, Thorlabs GmbH, Dachau/Munich, Germany) with a focal length of 2″. The IR beam (red color)

provided by the spectrometer was focused via the OAPM into the microfluidic IR-iHWG assembly. After propagating through the iHWG channel, IR radiation emanating at the distal end was guided to a liquid nitrogen cooled mercury-cadmium-telluride (MCT) detector (Fig. 3 **(D)**) (FTIR-16-2.00, Infrared Associates, USA). A syringe pump (New Era NE1010, New Era Pump Systems Inc., USA) provides a constant sample flow of 50 µL/min. Mixtures of absolute ethanol and MilliQ water are prepared beforehand using standard volumetric laboratory pipets.

During the measurements reported in the following, the EtOH and water concentration of different water/EtOH mixtures was investigated in the vapor phase at constant temperature of 20°C. For this purpose, different liquid mixtures are injected into the microfluidic channel using a syringe pump, and the vapor phase IR measurements were initiated.

Absorption bands in the EtOH molecule are classified in relation to O-H, C-H, C-O and C-C vibrations. For the evaluation of the present data, the C-H stretch vibration of the terminal CH_3- and of the CH_2 group is used.[14] After a baseline correction, the corresponding peak was integrated using integration boundaries from 3077-2567 cm^{-1}. All IR spectra were recorded in the spectral window of 4000 to 800 cm^{-1} at a spectral resolution of 2 cm^{-1} averaging 16 spectra per measurement resulting in a time resolution of approx. 20 s.

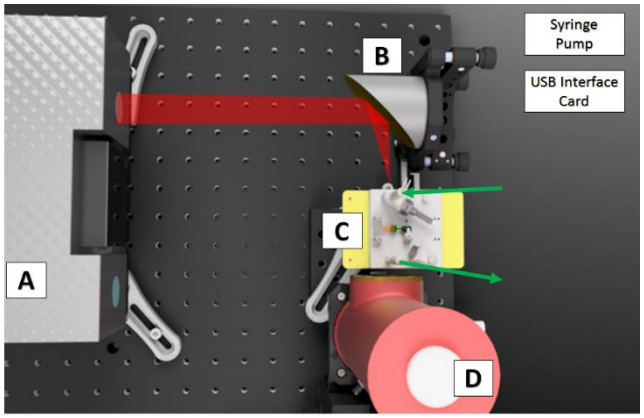

Figure 3: Schematic of the experimental setup comprising (A) FTIR spectrometer, (B) off-axis parabolic mirror, (C) microfluidic IR-iHWG assembly and (D) MCT detector. The red color indicates the IR beam and green arrows the gas stream.

CHARACTERIZATION OF THE MICROFLUIDIC IR-IHWG ASSEMBLY

In a first series of experiments, the microfluidic IR-iHWG assembly is characterized. The time period required for reaching vapor-liquid equilibrium is determined in order to estimate the achievable time resolution at present measurement conditions.

The microfluidic liquid channel is filled with pure EtOH, and then the iHWG is purged with N_2 for 10 min. After recording a background sample, four IR spectra are recorded within the N_2 stream. Then, IR spectra are continuously recorded after turning off the nitrogen gas stream (i.e., closed solenoid valves). After 2000 scans, the EtOH in themicrofluidic channel is exchanged with pure water, and the IR measurements are continued. For a precise evaluation of the residence time within the microfluidic IR-iHWG assembly, the number of averaged spectra is selected as 16 (i.e., one spectrum every 22.5 s).

ACTIVITY MEASUREMENTS OF ETOH SOLUTIONS

With the determined minimum evaporation and purging times, a six step protocol was developed for the measurement of different EtOH/water mixtures ranging from 0-100% EtOH in water in 10% increments. Table 1 summarizes the measurement procedure. During step 1, the channel of the iHWG is purged with nitrogen at a constant flow for 5 min ensuring complete gas exchange with nitrogen. In step 2, while the iHWG is still purged with N_2, a single channel background spectrum is recorded and later used as reference spectrum during sample measurements. During the sample injection phase (step 3), the liquid mixture is fed into the microfluidic channel. Step 4 corresponds to the measurement of four control spectra while purging the waveguide, yet, with sample already present within the microfluidic channel. Then, the purging gas stream is turned off during step 5, and IR measurements of sample vapors are initiated at step 6 while still perfusing the sample at 50 µL/min flow rate of.

In total, eleven EtOH-water-mixtures are investigated (cf. Figure S3 in the supporting information), and each mixture is analyzed three times. With increasing EtOH ratios in water, the vapor pressure of EtOH increases, which is detected in the vapor phase via the microfluidic IR-iHWG assembly.

Step	Time	Vapor cell content
1. Purging N2	5 min	N_2
2. Background	40 s	N_2
3. Sample injection	-	N_2
4. Control spectra	4 x 22.5 s	N_2
5. Stop purging N2	-	N_2
6. Measuring	12 x 25.5s	Sample vapor

Table 1. Measurement protocol: time consumption and description of vapor cell content.

RESULTS AND DISCUSSION

SYSTEM RESPONSE TIME

The overall response time of the system is determined as described in the experimental section. The temporal evolution of the EtOH integrated peak area is illustrated in Fig. 4A. Between 0 and 751 min, the evaporation of EtOH is continuously monitored. After 751 min, the liquid inside the microfluidic channel is exchanged with pure water. From 751-1500 min, spectra during the liquid exchange (from pure EtOH to 0% EtOH) are recorded.

The evaporation/diffusion kinetics are derived from the time required to completely fill or empty the iHWG channel with EtOH vapor.

First, the time needed for EtOH to reach a liquid/vapor equilibrium is determined. Once flushing the iHWG with nitrogen is stopped (i.e., after 4 control spectra), EtOH starts to evaporate and diffuses into the iHWG channel. Then, the EtOH integrated peak area exponentially with a response time of t_{90} = 134 s (Fig. 4B). Another important aspect is the time needed to completely exchange the volume within the iHWG channel by vapor from the exchanged liquid sample (i.e., here, water). The recovery time is evaluated as 269 s (t_r, Fig. 4C).

EVALUATION OF PHASE DIAGRAM USING THE MICROFLUIDIC IR-IHWG ASSEMBLY

Figure 5 (A) shows a comparison of the IR spectra of a 0% EtOH solution (red) and pure EtOH solution (black) in the spectral region between 3100-2700 cm^{-1}. In the red spectrum (0% EtOH), no absorptions are observed in the EtOH region of interest, while the black spectrum shows the typical absorption signature of a pure EtOH solution. Fig. 5 (B) illustrates the integrated peak area values for the various investigated solutions (black squares), and a comparison of the calculated activity values derived from these experiments with literature data (white circles).[15] In addition, the experimentally obtained data points are displayed with error bars, which were calculated as the standard deviation of the mean values (σ). For better readability, the error bars are magnified 5-fold, and are displayed with ±5σ.

Statistical variations within the experiments may be attributed to several factors including operational parameters (e.g., flow rate variations during background acquisition, not synchronized valve operations, etc.), pressure variations, temperature variations < 0.1°C, residual analyte vapor in the iHWG channel during RSC measurement, and condensation effects. Indeed, during our studies traces of condensation can be found on the FTIR spectra at high water concentration that will be dealt with in future generation of the device.

The correlation between absorbance and activity of the investigated EtOH solutions was obtained by dividing the observed peak areas by a constant which is calculated after equating the peak area of the 100% EtOH solution to one. Additionally, the literature values of a pure EtOH solution are set to one (i.e., activity of a pure solution is one). For this reason, the values determined in the present study appear slightly higher than the previously reported activity values derived from literature[11], but remain in excellent agreement.

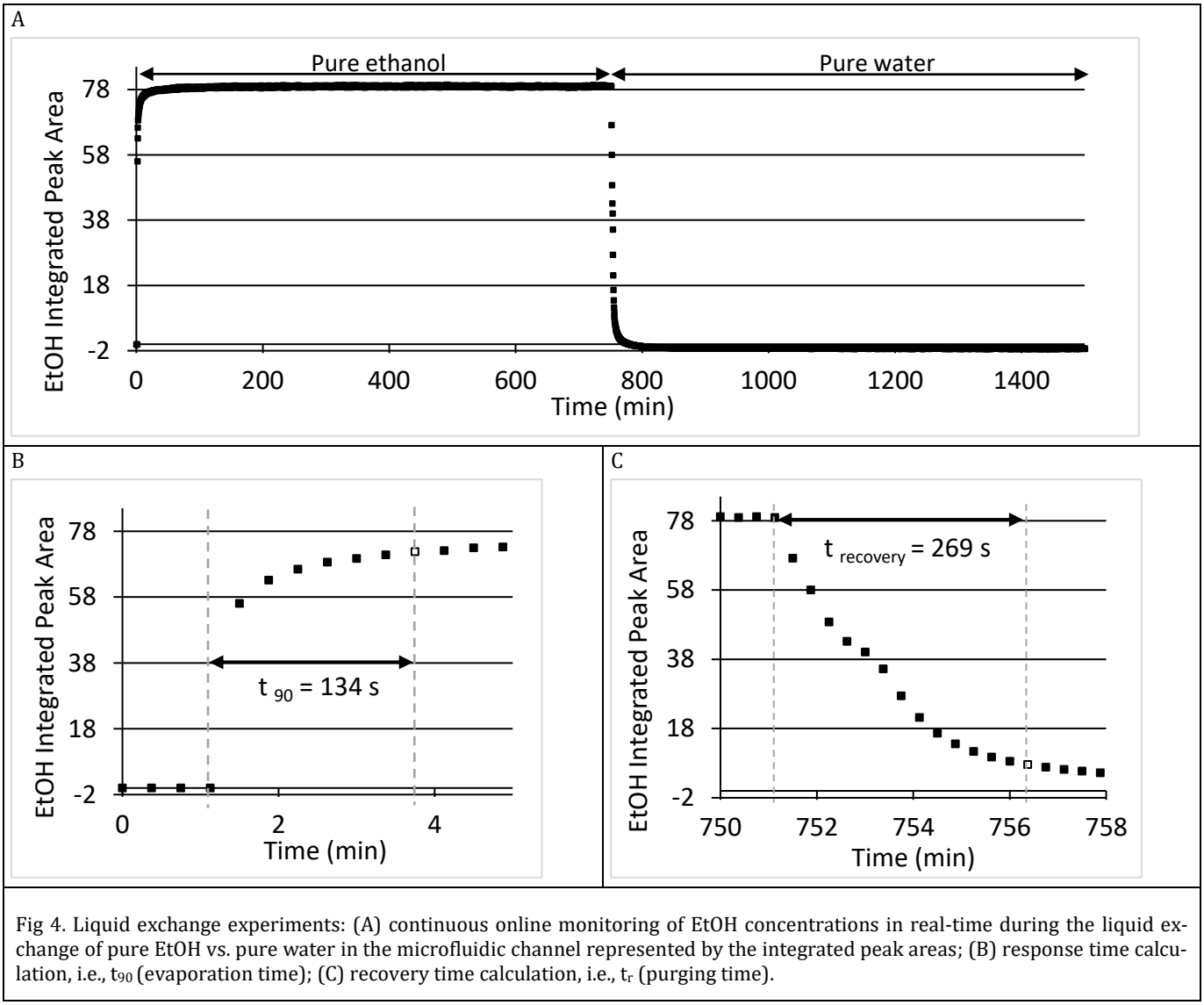

Fig 4. Liquid exchange experiments: (A) continuous online monitoring of EtOH concentrations in real-time during the liquid exchange of pure EtOH vs. pure water in the microfluidic channel represented by the integrated peak areas; (B) response time calculation, i.e., t_{90} (evaporation time); (C) recovery time calculation, i.e., t_r (purging time).

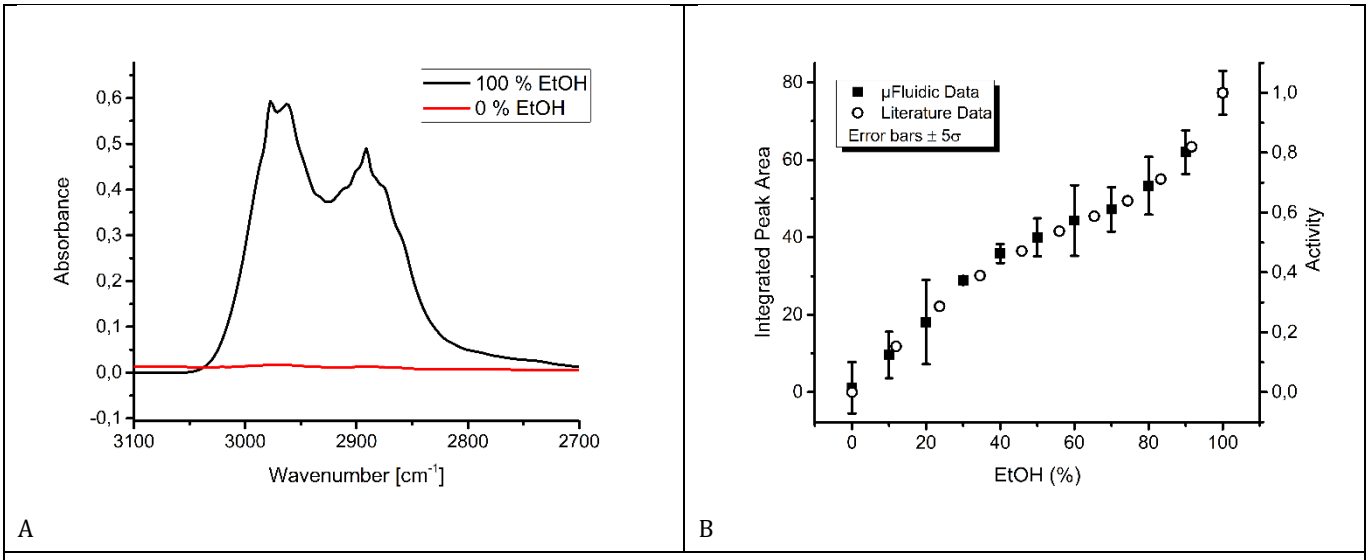

Fig 5. (A) Comparison of IR spectra of 0% (red) and pure EtOH (black) in the spectral region between 3100-2700 cm^{-1}, (B) Multi Y-Axis diagram with (black squares) the acquired integrated peak area values for the investigated data set (0-100% EtOH), and comparison of the experimentally obtained data with literature values[15,16] after conversion into activity values (white circles). Error bars are magnified 5-fold.

PHYSICOCHEMICAL BACKGROUND

At thermodynamic equilibrium between a liquid (l) and a vapor (v) phase at given pressure p, and temperature T, Gibbs energy G, is at a local minimum regarding mass transfer at the l/v interface,

$$(\mathrm{d}G/\mathrm{d}x_i)_{p,T} = 0,$$

Equation 1

where x_i denotes the mole fraction of compound i. At this condition, the chemical potential μ is equal in both phases,

$$\mu_{v,i} = \mu_{l,i}.$$

Equation 2

For non-ideal liquid mixtures in equilibrium with their vapor phase, the modified Raoult's law states that the compound activities $a_i(x_i) = \gamma_i x_i$ are linked to mole fractions x_i in the liquid phase, and y_i in the vapor phase:

$$\gamma_i x_i / p \; = \; \varphi_i y_i / p_i^{\mathrm{sat}}(T),$$

Equation 3

with the activity coefficient γ_i the temperature-dependent saturation vapor pressure $p_i^{\mathrm{sat}}(T)$ and the fugacity coefficient φ_i, which is equal to unity by assumption of ideal vapors. Furthermore, the Beer-Lambert law relates absorbance at a specific wavelength A_λ to compound concentration y_i as:

$$A_\lambda(y_i) = -\log\left(\frac{I(\lambda)}{I_0(\lambda)}\right) = \epsilon_\lambda l y_i,$$

Equation 4

with ϵ_λ as the molar attenuation coefficient, and l as the optical path length. Combining equations 3 and 4 yields:

$$a_i(x_i) = \gamma_i x_i = A_\lambda(y_i)\varphi_i \cdot \frac{p}{\epsilon_\lambda l p_i^{\mathrm{sat}}(T)} = A_\lambda(y_i)\varphi_i \cdot K.$$

Equation 5

As indicated, the remaining parameters may be combined into an instrumental and environmental factor K, which is constant if p and T are constant. Moreover, for a pure compound, activity is equal to one, $a = 1$, which is used for data calibration in the present study.

In consequence, as long as Beer's law holds true, equation 5 may be used to calculate the activity of any substance i, and alternatively, at a known mole fraction x_i. The activity coefficient of a compound may be derived via measuring its corresponding vapor phase absorbance at equilibrium conditions.

CONCLUSIONS AND OUTLOOK

The results presented herein demonstrate for the first time that a novel approach based on a microfluidic IR-iHWG assembly in combination with IR spectroscopy enables the determination of solution activities within different EtOH/water mixtures via vapor phase IR absorbance measurements. Furthermore, it is shown that iHWG structures readily combine with microfluidic technologies providing an integrated liquid phase sampling accessory for vapor phase studies. Based on the present results, the versatility of iHWGs previously demonstrated for the detection of environmentally/industrially relevant gases [17–20] and (bio)medically interesting analytes[21,22] may now be expanded towards vapor phase studies of liquids.

Following this conceptual demonstration, it is anticipated that microfluidic IR-iHWG assemblies establish an innovative approach for the evaluation of thermodynamic and kinetic data in more complex fluids encountered during various industrially relevant scenarios including but not limited to extraction, refining, distillation, agglomeration, etc.

Furthermore, using microfluidic IR-iHWG studies aids in better understanding the timely problem of mesoscale structuration and inhomogeneity in complex fluids, and potentially occurring supramolecular species (a.k.a., supramers)[23].

Last but not least, this analytical approach may enable to swiftly study processes based on complex fluids, thereby accelerating the development of sustainable processes and advanced process analysis/control technologies.

ASSOCIATED CONTENT

Supporting Information

The Supporting Information (PDF) is available free of charge on the ACS Publications website.

AUTHOR INFORMATION

Corresponding Authors

* BM: boris.mizaikoff@uni-ulm.de
* JCPG: jean-christophe.gabriel@cea.fr

Author Contributions

The manuscript was written through contributions from all authors. / All authors have given approval to the final version of the manuscript. / ‡ These authors contributed equally.

ACKNOWLEDGMENTS

JCG thanks (i) Prof. Thomas Zemb for discussions on initial chemical activity measurement issue and concept and general discussions on issues linked to chemical activity of solvent and initial concept; (ii) CEA Grenoble INAC institute for hosting his laboratory. The authors thank Christelle Laugier and Jean-Yves Laurent from CEA Grenoble (DRT/LITEN/DTNM) for gold layer sputtering and F. Né & V. Cachard from CEA Grenoble (DRT/D-OIC/SCSO) for milling equipment access.

Funding for JT and CP and research performed at CEA leading to these results has received funding from the European Research Council under the European Union's Seventh Framework Program (FP/2007-2013) / ERC Grant Agreement n. [320915] "REE-CYCLE": Rare Earth Element reCYCling with Low harmful Emissions. BM and JCG thank the Hubert Curien Program for bilateral traveling funding (PROCOPE n° 33104RC).

The Machine Shop at Ulm University is thanked for support during prototype development of the iHWG.

REFERENCES

(1) Bley, M.; Siboulet, B.; Karmakar, A.; Zemb, T.; Dufrêche, J.-F. *J. Colloid Interface Sci.* **2016**, *479*, 106–114.

(2) Zemb, T.; Bauer, C.; Bauduin, P.; Belloni, L.; Déjugnat, C.; Diat, O.; Dubois, V.; Dufrêche, J.-F.; Dourdain, S.; Duvail, M.; Larpent, C.; Testard, F.; Pellet-Rostaing, S. *Colloid Polym. Sci.* **2015**, *293* (1), 1–22.

(3) Schöttl, S.; Horinek, D. *Curr. Opin. Colloid Interface Sci.* **2016**, *22*, 8–13.

(4) Sturm, V.; Noll, R. *Appl. Opt.* **2003**, *42* (30), 6221.

(5) Castillo, P. C.; Sydoryk, I.; Gross, B.; Moshary, F. In *SPIE Defense, Security, and Sensing*; Vo-Dinh, T., Lieberman, R. A., Gauglitz, G. G., Eds.; International Society for Optics and Photonics, 2013; p 87180J.

(6) Griffith, D. W. T.; Leuning, R.; Denmead, O. T.; Jamie, I. M. *Atmos. Environ.* **2002**, *36* (11), 1833–1842.

(7) Esler, M. B.; Griffith, D. W.; Wilson, S. R.; Steele, L. P. *Anal. Chem.* **2000**, *72* (1), 206–215.

(8) Star, A.; Joshi, V.; Skarupo, S.; Thomas, D.; Gabriel, J.-C. P. *J. Phys. Chem. B* **2006**, *110*, 21014–21020.

(9) Gabriel, J.-C. P. *Comptes Rendus Phys.* **2010**, *11* (5–6), 362–374.

(10) Arcamone, J.; Niel, A.; Gouttenoire, V.; Petitjean, M.; David, N.; Barattin, R.; Matheron, M.; Ricoul, F.; Bordy, T.; Blanc, H.; Ruellan, J.; Mercier, D.; Pereira-Rodrigues, N.; Costa, G.; Agache, V.; Hentz, S.; Gabriel, J. C.; Baleras, F.; Marcoux, C.; Ernst, T.; Duraffourg, L.; Colinet, E.; Myers, E. B.; Roukes, M. L.; Andreucci, P.; Ollier, E.; Puget, P. *Tech. Dig. - Int. Electron Devices Meet. IEDM* **2011**, No. 5, 669–672.

(11) Wilk, A.; Carter, J. C.; Chrisp, M.; Manuel, A. M.; Mirkarimi, P.; Alameda, J. B.; Mizaikoff, B. *Anal. Chem.* **2013**, *85* (23), 11205–11210.

(12) Carter, J. C.; Chrisp, M. P.; Manuel, A. M.; Mizaikoff, B.; Wilk, A.; Kim, S.-S. *U.S. Pat. Appl. Publ.* **2013**.

(13) He, W.; Lv, W.; Dickerson, J. H. Springer, Cham, 2014; pp 9–17.

(14) Plyler, E. K. *J. Res. Natl. Bur. Stand. (1934).* **1952**, *48* (4), 281.

(15) O'Hare, K. D.; Spedding, P. L. *Chem. Eng. J.* **1992**, *48* (1), 1–9.

(16) O'Hare, K. D.; Spedding, P. L.; Grimshaw, J. *Dev. Chem. Eng. Miner. Process.* **2008**, *1* (2–3), 118–128.

(17) Petruci, J. da S.; Fortes, P.; Kokoric, V. *Sci. Rep.* **2013**, *3*

(September), 3174.
(18) Petruci, J. F. D. S.; Wilk, A.; Cardoso, A. A.; Mizaikoff, B. *Anal. Chem.* **2015**, *87* (19), 9605–9611.
(19) José Gomes da Silva, I.; Tütüncü, E.; Nägele, M.; Fuchs, P.; Fischer, M.; Raimundo, I. M.; Mizaikoff, B. *Analyst* **2016**, *141* (14), 4432–4437.
(20) Kokoric, V.; Widmann, D.; Wittmann, M.; Behm, R. J.; Mizaikoff, B. *Analyst* **2016**, *141* (21), 5990–5995.
(21) Kokoric, V.; Wilk, A.; Mizaikoff, B. *Anal. Methods* **2015**, *7* (9), 3664–3667.
(22) Seichter, F.; Wilk, A.; Wörle, K.; Kim, S.-S.; Vogt, J. a; Wachter, U.; Radermacher, P.; Mizaikoff, B. *Anal. Bioanal. Chem.* **2013**, *405* (14), 4945–4951.
(23) Kononov, L. O. *RSC Adv.* **2015**, *5* (58), 46718–46734.